Results from Modal Testing of the Daigneault Creek Bridge

Ann Sychterz[1], Ayan Sadhu[1], Sriram Narasimhan[1], Scott Walbridge[1]
[1]Department of Civil & Environmental Engineering, University of Waterloo

Abstract: Despite several full-scale applications in Canada, the vibrational characteristics and performance of aluminium pedestrian bridges have not been studied comprehensively in the literature. Currently, a specific pedestrian supplemental code for aluminium bridges does not exist; thus only the general AASHTO LRFD bridge design specifications need to be met. Field vibration data from full-scale pedestrian bridges would likely shed new light on their vibrational behaviour and performance. This will allow aluminium bridge designers to create a competitive alternative to bridges constructed with conventional materials. A field study was conducted during the fall of 2012 to estimate the modal characteristics of an aluminium bridge in Brossard, Québec. In this paper, the results of modal identification are presented, i.e., natural frequencies, damping, and mode shapes using a novel signal processing technique based on the vibration measurements. The estimated modal parameters are then compared with the results of a finite element model of the bridge. This field study provides new understanding of overall dynamics of aluminium pedestrian bridges, the contributions from higher modes, and the modal damping ratios.

Keywords: Pedestrian bridges, aluminium, modal identification, blind source separation, full-scale modelling.

1 Introduction

The estimation of natural frequencies, mode shapes, and modal damping of aluminium pedestrian bridges has not been extensively investigated. Vibrational characterization of pedestrian bridges has been undertaken for several well-known bridges that experienced unexpectedly high amplitude responses. The testing and analysis procedures are similar to those conducted for this study, though the Daigneault Creek Bridge is constructed from T6061 extruded aluminium. This 44 m clear span, 4 m wide, aluminium square hollow structural section, pony-truss bridge is the focus of this study. Behaviour of aluminium as a construction material is key to the further design of larger and higher occupancy aluminium bridges. Aluminium has a higher strength-to-weight ratio than steel for example, thus vibration control using damping is a key factor in the future work in this field.

Several of the well-known bridges were subjected to field tests for modal characterization, most notably the Millennium Bridge (Dallard 2001) the M-Bridge (Nakamura 2008), the Solférino bridge (Lenci et al. 2012), and the Ponte del Mare (Ceravolo 2011). The Millennium Bridge in London attracted public interest due to its large lateral displacements during its inauguration in 2000; assumed to be due to the pedestrian lock-in phenomenon (Dallard 2001). To address vibration concerns, 37 Taylor viscous dampers and 29 pairs of vertical tuned mass dampers (TMD) were installed along the bridge, with the ability to be individually disconnected (Pavic et al. 2002). Modal characterization tests used a vertical shaker, a horizontal shaker, and slotted bolted connections for these full-scale tests (Ceravolo 2004)(Chan et al. 2004). Shortly after the Millennium Bridge studies, an investigation on the Clifton Suspension Bridge in

England was performed (Macdonald et al. 2008). In this full-scale test, 27 modes less than 3 Hz were found, with most of those modes being either vertical or torsional. The main objectives in these studies were to understand the reasons for the large amplitude motions resulting from crowd loads.

The M-Bridge, Maple Valley Great Suspension Bridge, is a suspension bridge comprising of a reinforced concrete tower supporting a deck of two flexible steel H-girders, sway bracing, and steel grating (Kawasaki et al. 2009). For quick validation of the data, the modal frequencies and damping responses were calculated numerically on site for quick validation of their testing methods (Kawasaki et al. 2009). A 3-span pedestrian bridge at Texas Tech University connecting the campus to the football stadium was similar in design to the Millennium Bridge and experienced large amplitude vibrations from a crowd leaving a game. This pedestrian bridge was designed prior to the issuance of AASHTO LRFD bridge code for pedestrian bridges. Sampled at 30 Hz with tri-axial accelerometers, primary vibration was in torsional modes due to crowd loading (Landuyt 2012).

The Ponte del Mare is a suspension bridge over the Pescara River with two decks; an inner cyclist track and an outer pedestrian track. These tracks are secured with three viscous dampers, which were installed along the cables at the tower. Installed at mode-critical locations as predicted by the FE model, 8 piezoelectric accelerometers, sampled at 1000Hz, were placed on the bridge (Ceravolo 2011). Three types of 'output-only' identification methods were reported; Single Value Decomposition, Stochastic Subspace Identification (SSI), and Canonical Variate Analysis. However, the identification results suffered due to the nonstationarity of the data. Ambient Vibration Survey (AVS) to filter ambient noise has been implemented on other bridge tests, however it reduces data resolution that cannot be used for modal identification (Pavic 2002).

While pedestrian bridges have thus far been studied with an objective to understand the unexpected large motions, or to develop more refined load models, the objective of the current study is simply to perform a modal identification, and estimate the modal parameters of a full scale aluminium bridge; the Daigneault Creek aluminium pedestrian bridge in Brossard, Quebec. The vibration measurements on this bridge were obtained using twelve low-frequency, high-sensitivity, piezo-crystal accelerometers installed along the length of the bridge. Tests conducted included, but were not limited to: heel drop free vibration, single pedestrian walking, two pedestrian walking asynchronously, running, jumping, and cycling. The data was then transformed to the centreline of the bridge, with three degrees of freedom at each position along the bridge: lateral, vertical, and torsional acceleration. A finite element (FE) model using the design plans of the bridge was built. The resulting natural frequencies and mode shapes were compared against the results from a powerful modal identification signal processing technique (Sadhu 2011). It is anticipated that this will lead to a better characterization of aluminium bridges, and provide a test-bed for future studies by the group on load models for pedestrian bridges.

2 Full-Scale Instrumentation and Measurement Program

2.1 Structural Description of Daigneault Creek Bridge

In March 2012, MAADI Group installed Canada's longest aluminium pony truss bridge in Brossard, Quebec (Figure 1), for the City of Brossard. With a clear span of 44m, a height of 2.8 m, and a deck width of approximately 4m, the bridge connects a new subdivision from Rue Claudel to a major transportation and commercial area on Rue Grande Allée. The top and bottom girders are HSS 254x254 mm, the deck purlins are HSS 203.2x203.2 mm, and the deck diagonal bracing HSS 152.4x152.4 mm. Deck support, consisting of HSS 63x127 mm and HSS 127x127 mm, runs along the length of the pressure-treated Southern yellow pine deck. The bridge is fastened to the abutment on the side of Rue Claudel with slotted bolted connections into a cast in-place concrete shallow foundation.

Figure 1: Overall and underside pictures of the Daigneault Creek Bridge looking towards Rue Grande Allée

2.2 Details on Field Measurements

In October 2012, the Daigneault Creek Bridge was instrumented with twelve wired accelerometers. These PCB accelerometers model 393B31 were a piezo-crystal unit for low-frequency with a frequency range of 0.1Hz to 200 Hz for ±5\%, and a sensitivity of 10.0 V/g. The accelerometers had a single axis with an imposed positive direction such that the spatial orientation of the units along an axis had to be taken into account.

Each mounting block had an accelerometer in the lateral and vertical directions, where the longitudinal direction was neglected. The lateral accelerometers were installed on the inner faces of mounting block to the bridge deck. A pair of mounting brackets were installed on each of the bottom girders of the bridge at the locations L/4 (A), L/2 (B), and 3L/4 (C) (Figure 2).

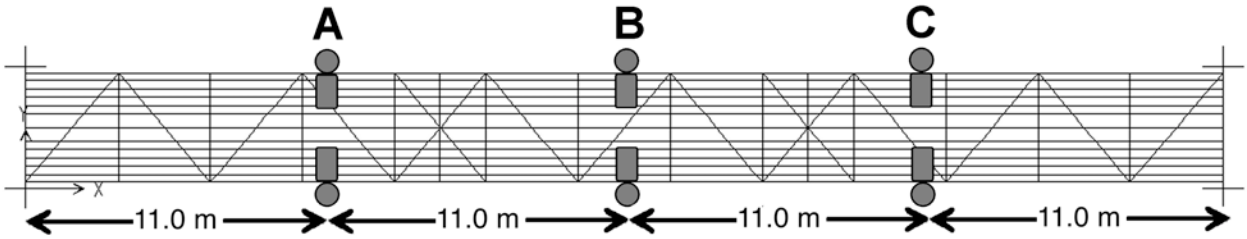

Figure 2: Plan view of PCB wired accelerometer locations installed on bridge girders

Each cluster on the above figure was a mounting bracket on the bridge comprised of a vertically (circle) and laterally (rectangle) aligned accelerometers. A custom-built, sandwich-style clamp from aluminium was used for mounting the sensors (Figure 3). Extensive ladder and rigging work were required to install the mounting brackets at location B due to the creek approximately 4 m below.

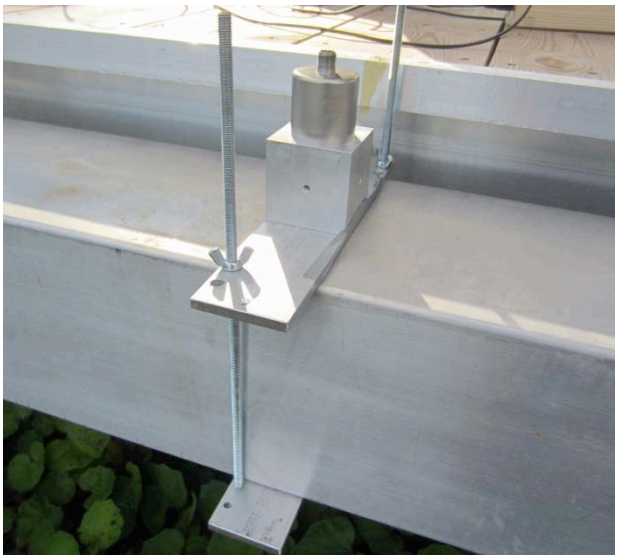

Figure 3: Installation of vertical accelerometer on the bottom square girder of the bridge using a sandwich-style clamp

The four accelerometers from each of the locations were fed into a PCB signal conditioner, and all channels were connected to a low-pass Butterworth filter set to a cut-off frequency equal to the sampling rate of 500 Hz. The signal from the filters was connected to a USB data acquisition system (manufactured by Datatranslation®) and a laptop running a data acquisition software for testing and measurement, Measure Foundry®. Various loading patterns were assessed during the field-testing such as walking, running, and jumping. Loading patterns are summarized in **Table 1**. The results from the first impulse test are sufficient for modal identification.

Table 1: Types of excitation used for field tests

Type	Description
Impulse	Heel drop at location A on north side of the bridge
	Heel drop at location B in the centre of the bridge
	Heel drop at location C on the south side of the bridge
	Jump from bottom railing at location A, B, and C on south side of the bridge
Single Pedestrian	Single pedestrian walking along centre and south side of the bridge
	Single pedestrian running along the centre and south side of the bridge
Pedestrian pair	Two pedestrians walking synchronously and asynchronously
Group Walking	Group of five walking synchronously and asynchronously
Vehicle	Cyclist driving over the bridge
	Car driving over the bridge

3 Analysis

In order to obtain preliminary estimates of the modal frequencies and shapes of the bridge prior to the commencement of the field studies, a finite element model was built (in a commercial program) using the design plans provided by the MAADI Group. All the elements were modelled using linear elastic frame elements (84 elements and 240 degrees of freedom), and the soil-structure interaction was neglected. The pedestrian railing was applied as a linearly distributed dead load of 1.2 kN/m as per the design drawing. The supports were assumed to be pinned joints (safe assumption for short-term operational loads). A powerful signal-processing algorithm, called Second-order Blind Identification (SOBI), was employed for processing the measurements and to obtain the modal parameters. The data presented here could be processed through a variety of other methods (e.g., SSI), perhaps with equally reliable results. However, SOBI was selected primarily because the class of methods on which SOBI is based

provides a flexible framework to process data from the narrowband excitations tested (running, walking, etc.). Analysis using other methods is beyond the scope of this paper.

3.1 Second-Order Blind Identification

The basic equations for the signal processing technique used are presented. Consider a linear, classically damped, and lumped-mass n degrees-of-freedom structural system, subjected to an excitation force, $\mathbf{F}(t)$:

[1] $$\mathbf{M}\ddot{\mathbf{x}}(t) + \mathbf{C}\dot{\mathbf{x}}(t) + \mathbf{K}\mathbf{x}(t) = \mathbf{F}(t)$$

where, $\mathbf{x}(t)$ is a vector of displacement coordinates at the degrees of freedom. $\mathbf{M}$, $\mathbf{C}$, and $\mathbf{K}$ are the mass, damping, and stiffness matrices of the multi-degree-of-freedom system. The solution to [1] can be written in terms of modal superposition of vibration modes with the following matrix form (Antoni 2005)(Sadhu 2011):

[2] $$\mathbf{x} = \Psi\mathbf{q}$$

where, $\mathbf{q}$ is a matrix of the corresponding modal coordinates, and $\Psi_{n\times N}$ is the modal transformation matrix. Under the conditions where the modal coordinates are mutually uncorrelated with non-similar spectra, the normal coordinates can be regarded as the most uncorrelated sources (Antoni 2005)(Sadhu 2011). The basic framework of second-order blind identification (SOBI) (Belouchrani et al. 1997) is the simultaneous diagonalization of two covariance matrices $\mathbf{R}_\mathbf{x}(0)$ and $\mathbf{R}_\mathbf{x}(p)$ evaluated at the time-lag zero and *p*, respectively. This can be written as:

[3] $$\begin{aligned}\mathbf{R}_\mathbf{x}(0) &= E\{\mathbf{x}(n)\mathbf{x}^T(n)\} = \mathbf{A}\mathbf{R}_\mathbf{s}(0)\mathbf{A}^T \\ \mathbf{R}_\mathbf{x}(p) &= E\{\mathbf{x}(n)\mathbf{x}^T(n-p)\} = \mathbf{A}\mathbf{R}_\mathbf{s}(p)\mathbf{A}^T\end{aligned}$$

where:

[4] $$\mathbf{R}_\mathbf{s} = E\{\mathbf{s}(n)\mathbf{s}^T(n-p)\}$$

The following three steps set up the essence of SOBI: whitening, orthogonalization, and unitary transformation. Whitening is a linear transformation in which, $\mathbf{R}_\mathbf{x}(0) = \left(1/N\right)\left(\sum_{n=1}^{N}\mathbf{x}(n)\mathbf{x}^T(n)\right)$ using singular value decomposition, $\mathbf{R}_\mathbf{x}(0) = \mathbf{V}_\mathbf{x}\Lambda_\mathbf{x}\mathbf{V}_\mathbf{x}^T$ where $\Lambda_\mathbf{x}$ and $\mathbf{V}_\mathbf{x}$ are the eigenvalues and eigenvectors of the co-variance matrix of $\mathbf{R}_\mathbf{x}(0)$ respectively. Then, the standard whitening is realized by a linear transformation expressed as:

[5] $$\bar{\mathbf{x}}(n) = \mathbf{Q}\mathbf{x}(n) = \Lambda_\mathbf{x}^{-\frac{1}{2}}\mathbf{V}_\mathbf{x}^\mathbf{T}\mathbf{x}(n)$$

Because of whitening, $\mathbf{R}_\mathbf{x}(p)$ becomes $\mathbf{R}_{\bar{\mathbf{x}}}(p)$, which is given by the equation:

[6] $$\mathbf{R}_{\bar{\mathbf{x}}}(p) = \left(1/N\right)\left(\sum_{n=1}^{N}\mathbf{x}(n)\mathbf{x}^T(n-p)\right) = \mathbf{Q}\mathbf{R}_\mathbf{x}(p)\mathbf{Q}^T$$

Using the [6] and [3], we get:

[7] $\mathbf{R}_{\bar{\mathbf{x}}}(p) = \mathbf{QAR}_S(p) = \mathbf{A}^T\mathbf{Q}^T$

The above equation states that by diagonalizing the whitened covariance matrix at a particular time-lag, the unitary matrix product $\mathbf{QA}$ can be determined, resulting in the mixing matrix, $\mathbf{A}$. This process of diagonalization is implemented numerically, and typically involves jointly diagonalizing several covariance matrices at a given lag p (Belouchrani et al. 1997). The second step, called orthogonalization, is applied to diagonalize the matrix $\mathbf{R}_{\bar{\mathbf{x}}}(p)$ whose eigenvalue decomposition satisfies:

[8] $\mathbf{V}_{\bar{\mathbf{x}}}\mathbf{R}_{\bar{\mathbf{x}}}(p)\mathbf{V}_{\bar{\mathbf{x}}}^T = \Lambda_{\bar{\mathbf{x}}}$

Since the diagonal matrix $\Lambda_{\bar{\mathbf{x}}}$ has distinct eigenvalues, it is easy to see that the product $\mathbf{QA}$ is a unitary matrix, and the mixing matrix can be estimated by the equation:

[9] $\hat{\mathbf{A}} = \mathbf{Q}^{-1}\mathbf{V}_{\bar{\mathbf{x}}} = \mathbf{V}_{\mathbf{x}}\Lambda_{\mathbf{x}}^{\frac{1}{2}}\mathbf{V}_{\bar{\mathbf{x}}}$

where $\hat{\mathbf{A}}$ is the estimated mixing matrix of $\mathbf{A}$. The problem now becomes one of unitary diagonalization of the correlation matrix $\mathbf{R}_{\bar{\mathbf{x}}}(p)$ at one or several non-zero time lags. The determination of the unitary matrix is carried out using a numerical procedure, commonly known as joint approximate diagonalization (Belouchrani et al. 1997). Denoting $\mathbf{V} = \mathbf{QA}$, $\mathbf{D} = \mathbf{V}^T\tilde{\mathbf{R}}_{\bar{\mathbf{x}}}(p)\mathbf{V}$, the problem is one of finding the minimum of the performance index J given by:

[10] $J(\mathbf{V},\mathbf{p}) = \sum_p \sum_{1\le i\ne j\le n} \left|D_{ij}^p\right|^2$

Then, the unitary matrix $\mathbf{V}$ corresponding to minimum J over fixed h iterations is said to be an approximate joint diagonalizer (Belouchrani et al. 1997). Once $\hat{\mathbf{A}}$ is estimated, the sources $\mathbf{s}$ can be estimated using the pseudo-inverse of [1]:

[11] $\hat{\mathbf{s}} = \hat{\mathbf{A}}^{-1}\mathbf{x}$

4 Results

4.1 Results from the FE model

As mentioned earlier, the results discussed in this section correspond to the heel drop at location A. Due to the relatively light-weight of the bridge, it is expected that this type of excitation would be able to excite all the dominant modes of the bridge. The high-sensitivity accelerometers together with the signal conditioning and filters resulted in acceleration measurements with relatively low noise. Hence, no pre-processing was required prior to conducting the analysis. The finite element model was used to conduct a linear eigenvalue analysis of the assembled mass and stiffness matrices. These eigenvalues correspond to the natural frequencies, and the eigenvectors to the mode shapes. While the lower frequencies usually dominate the response of building structures, typically for pedestrian bridges, these consist of a range of frequencies distributed in a relatively narrow bandwidth. The lowest frequency corresponds to lateral-torsion, the second lowest frequency causes a first mode vertical movement, and the third lowest

frequency causes a combined vertical-torsional movement. These are shown in Figure 4, while all the frequencies resulting from the model are summarized together with the identification results next.

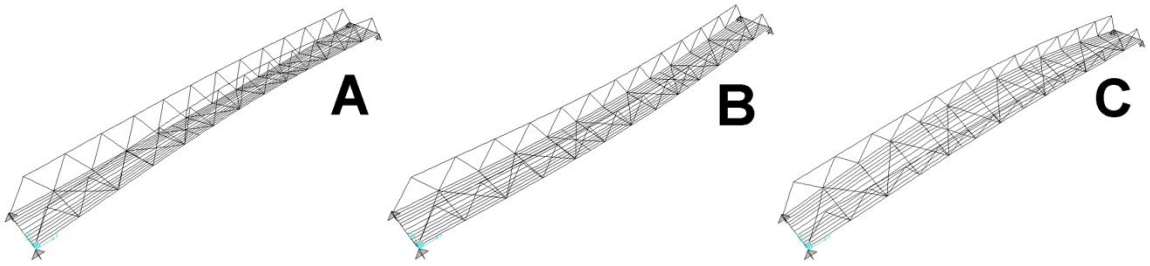

Figure 4: Finite element first mode shape for [A] 3.1 Hz lateral-torsional, [B] 3.4 Hz vertical, and [C] 5.6 Hz vertical-torsional

4.2 Output-only modal identification results

In order to estimate the modal information, the SOBI method (Belouchrani et al.1997) was implemented to extract the individual modal frequencies, damping ratios, and the corresponding mode shapes. Mode shapes are derived from the mixing matrix, which delineates the order of the mode by period of the sine curve fitting through the data. The sources, separated using SOBI, were transformed to the frequency domain to clearly observe the frequencies. One of the main observations in the results is that not all sources were mono-component; the ones that were found to be mono-component are shown in Figure 5.

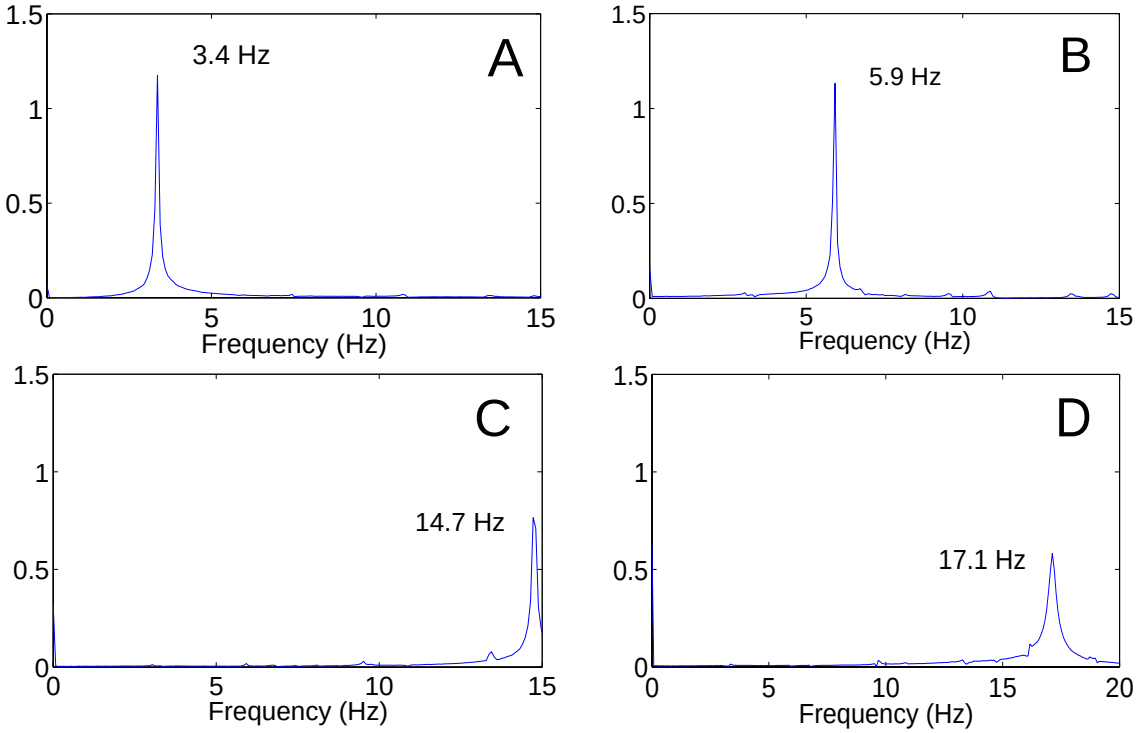

Figure 5: Frequency-domain of clean separated signals of [A] 3.4 Hz, [B] 5.9 Hz, [C] 14.7 Hz, and [D] 17.1 Hz

While some of the sources were found to be mono-component, other sources were not successfully delineated; such sources are shown in Figure 6. Though the individual frequencies are clearly identified in the sources, they are not mono-component. The mode shapes corresponding to these modes cannot be separated from the measurements. This process is known as mode-mixing and the occurrence of this can be explained as follows.

Considering equation [2], one of the main conditions for SOBI is that the matrix $\Psi_{n\times N}$ is full-rank. That is, the number of measurements is at least equal to or greater than the number of sources to be identified. This is known as the *over-determined* case. In practice, the number of sensors should be definitely larger than the sources to be identified else it is an *under-determined* case. In the context of the problem at hand, due to the relative light-weight of the bridge, several modes were excited. As can be seen from Figures 4 and 5, nearly 10 modes are excited, while only 12 sensors were deployed. This resulted in several sources mixed with others, and SOBI being unable to separate successfully. Hence, only the frequencies can be separated using this method, but not the mode shapes or the damping ratios. In order to successfully separate the mode shapes and damping ratios, other signal processing tools will have to be employed (Hazra et. al 2012). However, SOBI was able to clearly delineate four sources along with their associated mode shapes and damping ratios, and the complete set of results are presented.

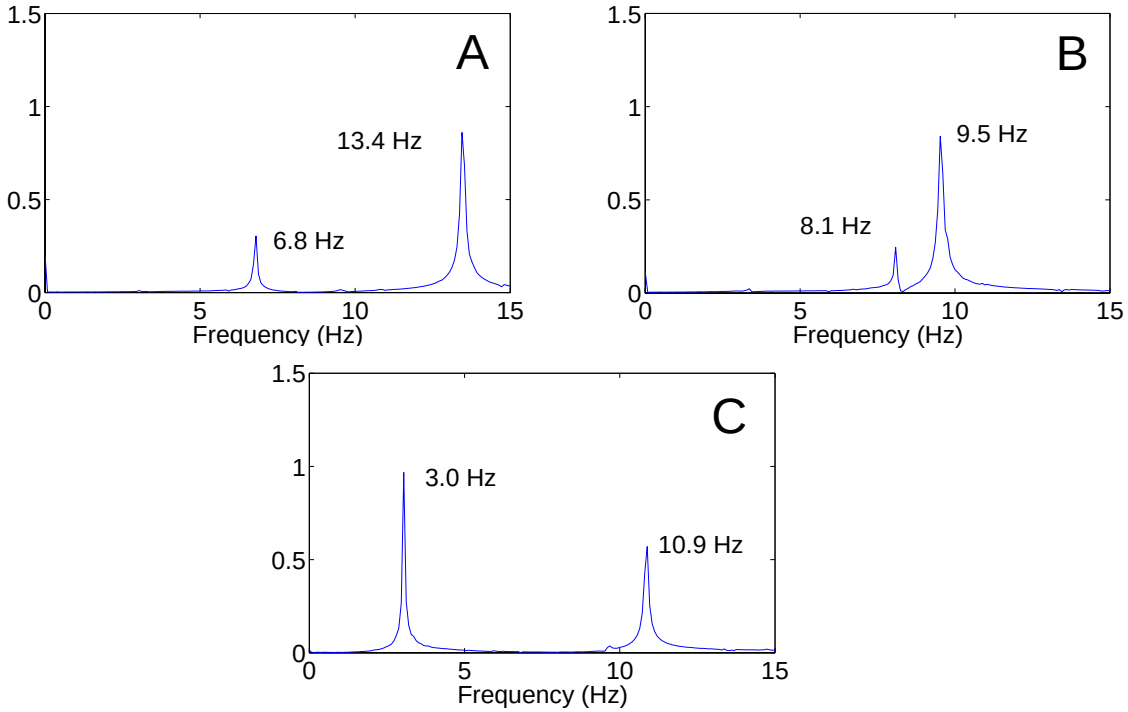

Figure 6: Frequency-domain of mixed low-energy signals at [A] 6.8 Hz and 13.4 Hz, [B] 8.1 Hz and 9.5 Hz, and [C] 3.0 Hz and 10.9 Hz

4.2.1 Estimated modal parameters

Only four sources were found to be mono-component. These correspond to 3.4 Hz (vertical), 5.9 Hz (vertical-torsional), 14.7 Hz (torsional) and 17.1 Hz (lateral mode of the truss sides). The mode shapes were plotted corresponding to these sources (Figure 7). The lowest mode, 3.0 Hz, was mixed with the 13.4 Hz, and hence only the frequency and not the mode shape was estimated clearly, which is compared to the predicted frequencies (Table 2). Most of the FE model predictions are within acceptable range to the parameters determined from the collected data.

Table 2: Comparison of SOBI and FE model results for natural frequencies

FE Model (Hz)	3.0	3.4	5.6	7.2	7.5	9.5	10.9	13.6	14.8	16.8
SOBI (Hz)	3.0	3.4	5.9	6.8	8.1	9.5	10.9	13.4	14.7	17.1

The damping estimates for the mono-component sources are tabulated in Table 3. Since the sources are mono component, each source was treated as mono-component source, and an exponential decay curve was fitted to the data, which resulted in the tabulated damping values. All the damping values are around or less than 1% critical; however, these results must be interpreted with caution as damping values tend to exhibit significant uncertainty and are often amplitude dependent. Hence, these results should provide preliminary estimates, and a thorough statistical analysis is not presented.

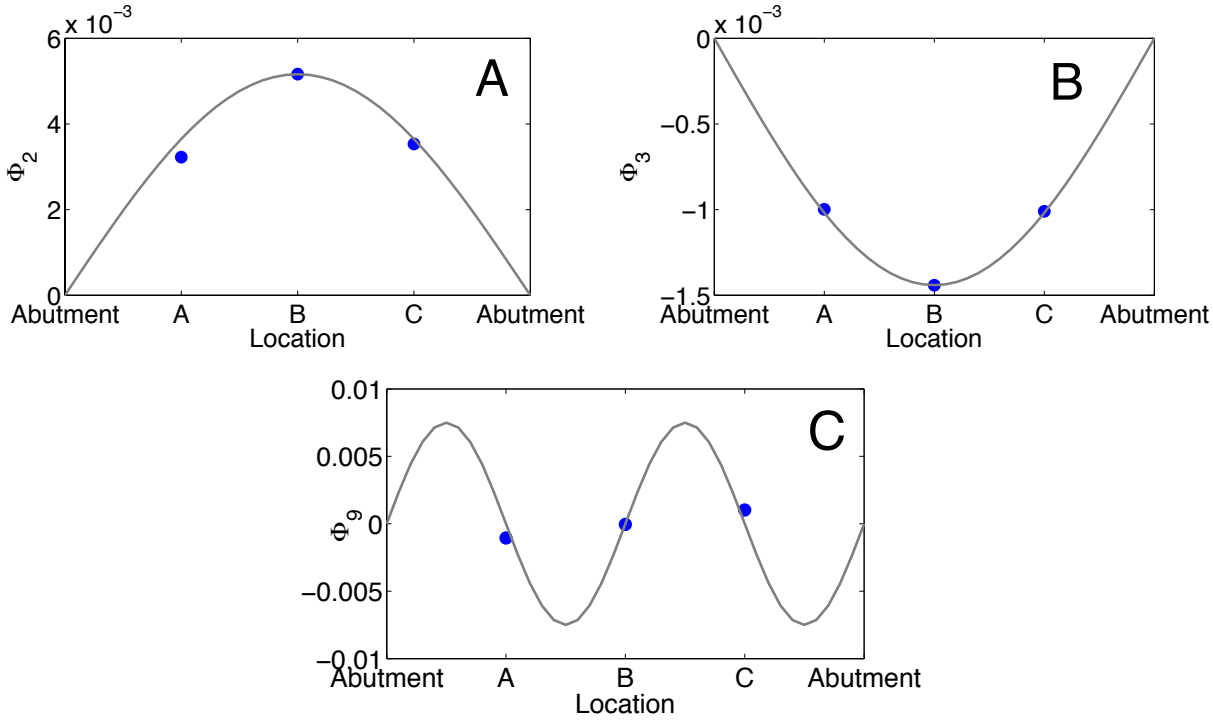

Figure 7: Mode shapes for [A] 3.0 Hz vertical, [B] 5.9 Hz vertical-torsional, and [C] 14.7 Hz torsional

Table 3: Observed data and damping results from SOBI analysis

Mode	Frequency (Hz)	Damping (%)
1	3.3	1.2
2	5.9	0.6
3	14.7	0.9
4	17.1	1.1

4.2.2 Response measurements

The acceleration measurements provided a clear indication regarding the level of vibrations recorded in the bridge to various loading conditions. The Canadian Highway Bridge Code (Commentary on CAN/CSA-S6- 06, Canadian Highway Bridge Design Code) recommends checking values for a single pedestrian (weighing 700 N) against the serviceability criteria set forth in their commentary. A modal analysis approach revealed that the maximum accelerations due to a single pedestrian was approximately 0.4 m/s^2, which is well within the acceptable range of approximately 0.6 m/s^2. As revealed by the recorded responses near the centre of the bridge in Figure 8[A], the maximum acceleration is approximately 0.25 m/s^2 for a single individual walking on the bridge. For a group of five pedestrians walking randomly (Figure 8[B]), the maximum acceleration increases to approximately 0.5 m/s^2. Due to space limitations, more discussion and results from field measurements cannot be included in this paper.

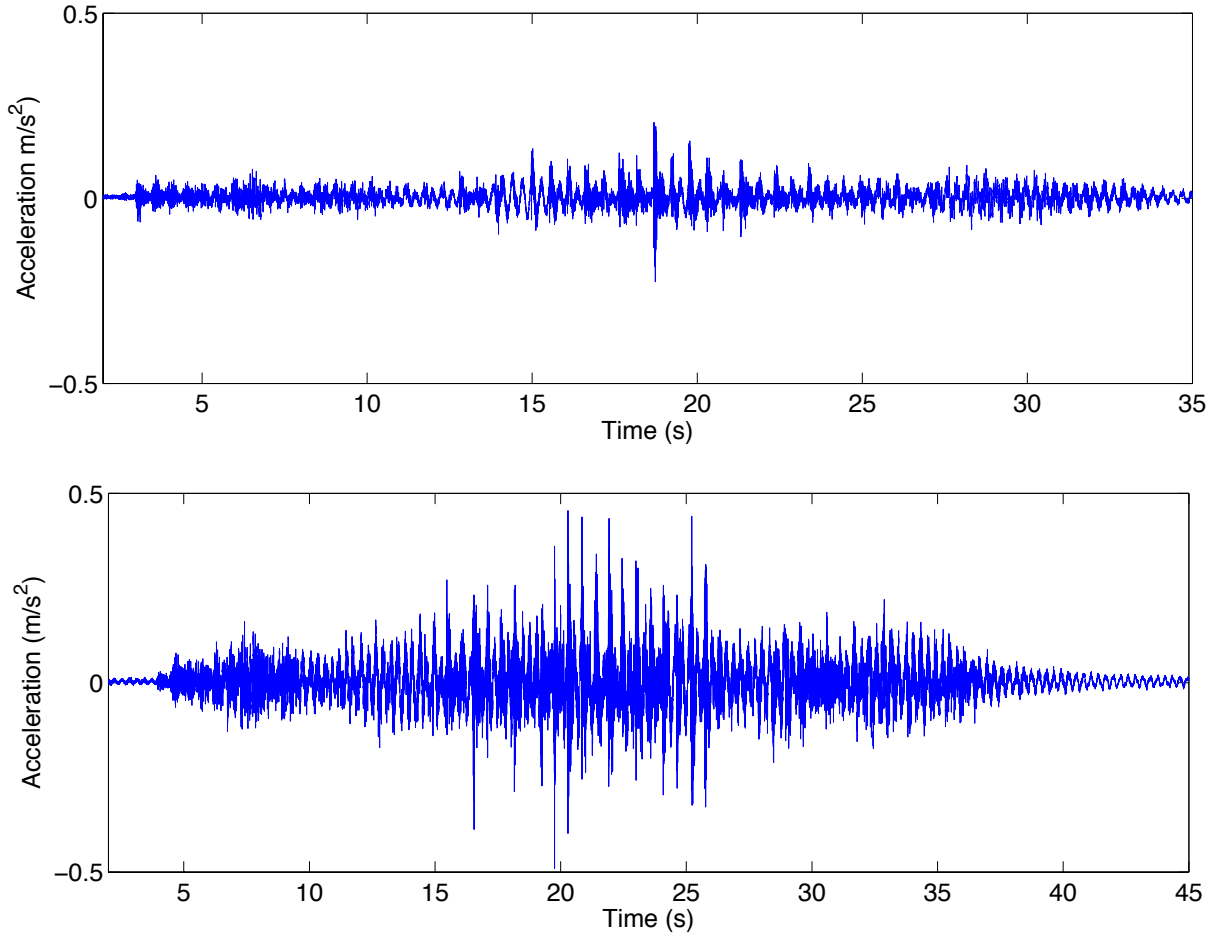

Figure 8: Response at location B (centre) of the bridge for [A] a single person walking and [B] group of 5 people walking

5 Summary and ongoing work

Results from the finite element model of the Daigneault Creek Bridge correlated well with the estimated natural frequencies estimated using SOBI. Due to the relative flexibility of the bridge, it was possible to excite several modes from a heel drop test, which resulted in the density of sensors being insufficient for treatment using traditional SOBI. Nevertheless, SOBI provided good estimates for most of the natural frequencies of the bridge, the mode shapes and damping ratios for four modes.

There is ongoing work to characterize the levels of vibrations during other tests, and extensions to SOBI that can address the shortcomings observed in this method. These methods include under-determined extensions to SOBI, which will alleviate the issue of mode mixing and will help delineate all the modes with the same number of sensors. Further studies and analysis is currently underway to use this data to develop reliable load models to predict responses of flexible aluminium bridges to individual pedestrian as well as crowd loading.

6 Acknowledgments

The authors would like to thank Alex de la Chevrotière of MAADI Group and Jacques Internoscia from the Aluminium Association of Canada for providing support and funding to complete a vibration characterization of the Daigneault Creek aluminium pedestrian bridge. Field work would not have been possible without the help of Richard Morrison and Pampa Dey from the University of Waterloo.

7 References

P. Reynolds A. Pavic, T. Armitage and J. Wright. Methodology for modal testing of the Millennium bridge, london. *Structures and Buildings,* 152:111–121, May 2002.

J. Antoni. Blind separation of vibration components: Principles and demonstrations. *Mechanical Systems and Signal Processing,* 19:1166–1180, 2005.

A. Belouchrani, K. Abed-Meraim, J.F. Cardoso, and E. Moulines. A blind source separation technique using second-order statistics. *IEEE Transactions on signal processing,* 45(2):434–444, 1997.

R. Ceravolo. Use of instantaneous estimators for the evaluation of structural damping. *Journal of Sound and Vibration,* 274:385–401, May 2004.

Pat Dallard. London Millennium bridge: Pedestrian-induced lateral vibration. *Journal of Bridge Engineering,* 6:412–417, December 2001.

Dean Van Landuyt, Delong Zuo, and Jieying Hua. A model of pedestrian-induced bridge vibration based on a full scale model. *Engineering Structures,* 45:117–126, June 2012.

B. Hazra, A. Sadhu, A.J. Roffel, P.E. Paquet, and S. Narasimhan. Underdetermined blind identification of structures by using the modified cross-correlation method. *Journal of Engineering Mechanics,* 138(4):327–337, 2012.

Stefano Lenci and Laura Marcheggiani. On the dynamics of pedestrians-induced lateral vibrations of footbridges. *Nonlinear Dynamic Phenomena in Mechanics,* 181:63–114, 2012.

J.H.G Macdonald. Pedestrian-induced vibrations of the Clifton Suspension bridge, UK. *Bridge Engineering,* 161(BE2):69–77, June 2008.

A. Pavic, M. Willford, P. Reynolds, and J. Wright. Key results of modal testing of the Millennium Bridge, London. 2002.

Giuseppe Abbiati Anil Kumar Rosario Ceravolo, Nicola Tondini. Dynamic characterization of complex bridge structures with passive control systems. *Structural Control and Health Monitoring,* 19:511–534, February 2012.

A. Sadhu, B. Hazra, S. Narasimhan, and M. D. Pandey. Decentralized modal identification using sparse blind source separation. *Smart Materials and Structures,* 20(12):125009, 2011.

Hiroshi Katsuura, Kaoru Yokoyama, Shunichi Nakamura, and Toshitsugu Kawasaki. Experimental studies on lateral forces induced by pedestrians. *Journal of Constructional Steel Research,* 64:247–252, May 2008.

Toshitsugu Kawasaki, and Shunichi Nakamura. A method for predicting the lateral girder response of footbridges induced by pedestrians. *Journal of Constructional Steel Research,* 65:1705–1711, March 2009.

S.L. Chan, S.S. Law, and Z.M. Wu. Vibration control study of a suspension footbridge using hybrid slotted bolted connection elements. *Engineering Structures,* 26:107–116, September 2004.